Available online at www.sciencedirect.com
SCIENCE DIRECT®
Physica C 426–431 (2005) 699–704
PHYSICA C
www.elsevier.com/locate/physc

# Database for thermal and mechanical properties of REBaCuO bulks

Hiroyuki Fujishiro [a,*], Kazumune Katagiri [a], Akira Murakami [b], Yasuhiro Yoshino [a], Koshichi Noto [a,c]

[a] *Faculty of Engineering, Iwate University, 3-4-5 Ueda, Morioka 020-8551, Japan*
[b] *Hirosaki University, 3 Bunkyo-cho, Hirosaki 036-8561, Japan*
[c] *Iwate Industrial Promotion Center, 3-35-2 Iiokashinden, Morioka 020-0852, Japan*

Received 23 November 2004; accepted 24 January 2005
Available online 14 July 2005

**Abstract**

The thermal properties (thermal conductivity, thermal diffusivity, thermoelectric power, thermal dilatation, etc.) and the mechanical properties (Young's modulus, strength, hardness, fracture toughness, etc.) have been measured at low temperatures (4–300 K) and under a high magnetic field (0–10 T) for about 50 REBaCuO bulks (RE = Y, Gd, Nd, Sm, Dy, etc.). We have constructed the database of these properties and opened it on the Web site (thermal properties: http://ikebehp.mat.iwate-u.ac.jp/database.html and mechanical properties: http://paris.mech.iwate-u.ac.jp/sc-bulk/database.html). The influence of the species of RE ions, the content, size and dispersion of the RE211 (or Nd422) phase and Ag particles and the defects distribution on these properties is characterized.


*PACS:* 74.72.−h; 51.20.+d; 74.70; 62.20.Mk

*Keywords:* REBaCuO bulk; Thermal properties; Mechanical properties; Database; Low temperature; Applied field

## 1. Introduction

For the practical applications and fundamental researches of the melt-processed REBaCuO superconductors (RE: rare earth elements), thermal properties such as the thermal conductivity, thermal dilatation, etc. and the mechanical properties such as the Young's modulus, strength, hardness, etc. are valuable parameters besides the electromagnetic properties such as the critical current density $J_c$ and the trapped magnetic field $B_T$. The REBaCuO bulk material is an anisotropic and complex material, which consists of RE123, RE211, Ag and Pt. The thermal and mechanical

* Corresponding author. Tel./fax: +81 19 621 6363.
*E-mail address:* fujishiro@iwate-u.ac.jp (H. Fujishiro).

0921-4534/$ - see front matter © 2005 Elsevier B.V. All rights reserved.
doi:10.1016/j.physc.2005.01.045

properties depend on the quality and alignment of the RE123 superconducting phase, and the content, size and dispersion of the RE211 phase and added metals. Defects such as voids and cracks are also the influencing factors, especially, for the mechanical properties. We have measured the thermal and mechanical properties at low temperatures (4–300 K) and under a high magnetic field (0–10 T) for REBaCuO bulks, which were fabricated by several companies and institutes. We have constructed the database of these properties and opened it on the Web site. In a conventional database for materials, the numerical data and figures are aligned boringly for each sample. In order to make the origin of these properties clear and to elucidate the relation between the samples, we have constructed the new type database, which is named as the ''advanced database'', together with the data for each sample with a conventional style. In this paper, we introduce the database for thermal and mechanical properties of HTSC bulks. The typical origin of these properties is discussed.

## 2. Experimental

The REBaCuO superconducting bulk samples (RE = Y, Sm, Nd, Gd, Dy, Ho and (Nd, Eu, Gd)) were fabricated at DOWA Mining Co. Ltd. (DOWA), Nippon Steel Co. Ltd. (NSC) and International Superconductivity Technology Center, Superconductivity Research Laboratory (ISTEC). Table 1 summarizes the specifications of the bulk samples investigated in this study. The content of the RE211 phase (or Nd422 phase) to the RE123 phase was expressed as RE123:RE211 = 100:$X$. The Pt powder of 0.4–0.5 wt.% was added in all the samples.

The thermal conductivity $\kappa(T)$ and thermoelectric power $S(T)$ were measured by a steady-state heat flow method and the thermal diffusivity $\alpha(T)$ was measured by an arbitrary heating method under an identical experimental setup with the $\kappa$ and $S$ measurements [1]. The specific heat $C(T)$ was estimated from the relation $C = \kappa/\alpha$. The thermal dilatation $\Delta L(T)/L(300\ K)$ was measured using a strain-gage method [2]. All the thermal properties were measured in the *ab*-plane and along the *c*-axis using a Gifford–McMahon (GM) cycle helium refrigerator as a cryostat between 4 and 300 K. The magnetic field of up to 10 T was applied using a cryocooler-cooled superconducting magnet [3].

Tensile, bending and compressive tests were carried out at the cross-head speed of 0.15 mm/min by using the 2 kN Shimadzu Servopulser or the 5 kN Shimadzu Autograph testing machine equipped with loading jigs. The tensile test specimen, $3 \times 3 \times 4\ mm^3$in size, glued to the aluminum alloy rods were loaded through the universal joints. The bending test was carried out using three-point bending specimen, $4 \times 3 \times 36\ mm^3$ in size with the fulcrum span 30 mm. The dimensions of the compressive test specimen were $3 \times 3 \times (8$ or $12)\ mm^3$. The fracture toughness tests were

Table 1
Specifications of the bulk samples investigated in this study

| Company and Institute | RE element | (123):(211) = 100:X | Ag content (wt.%) | Atmosphere during growth | Measuring direction |
|---|---|---|---|---|---|
| DOWA | Y | $X$ = 33–40 | 0–15 | In air | *ab* and *c* |
| | Sm | $X$ = 10–40 | 0–20 | In air | *ab* and *c* |
| | Gd | $X$ = 40 | 10–15 | In air | *ab* and *c* |
| NSC | Y | $X$ = 0–33 | 0 | In air | *ab* and *c* |
| | Gd | $X$ = 33–50 | 10 | In air | *ab* and *c* |
| | Dy | $X$ = 33 | 0 | In air | *ab* and *c* |
| ISTEC | Nd | $X$(422) = 20–30 | 0–10 | Reduced $O_2$ | *ab* |
| | Gd | $X$ = 50 | 0–30 | Reduced $O_2$ | *ab* |
| | Dy | $X$ = 5–40 | 0–10 | In air | *ab* |
| | Ho | $X$ = 40 | 10 | In air | *ab* |
| | (Nd,Eu,Gd) | $X$ = 11–43 | 0–20 | Reduced $O_2$ | *ab* |

conducted using three-point bending specimens $4 \times 3 \times 18\ mm^3$ in size containing single edge V-notch. Indentation tests were carried out by using the Vickers hardness testing machine equipped with the GM cryocooler [4].

## 3. Results and discussion

The database for each sample can be accessed from the following Web sites: (http://ikebehp.mat.iwate-u.ac.jp/database.html) and (http://paris.mech.iwate-u.ac.jp/sc-bulk/database.html). In this section, we introduce the characteristic "advanced database" in which the origin of these properties can be clarified.

### 3.1. Thermal properties [1–3,5–9]

Fig. 1 shows the temperature dependence of the *ab*-plane thermal conductivity $\kappa_{ab}(T)$ for various kinds of bulks with the RE211 contents of $X = 40$, adding the $Ag_2O$ of 10 wt.%. The thermal conductivity $\kappa_c(T)$ along the *c*-axis for the Gd- and Sm-system is also shown. In the previous paper, it was confirmed for all the RE systems that the absolute value of $\kappa_{ab}(T)$ decreased with increasing $X$ and increased with increasing content of the high-thermal-conductive Ag [3,9]. The anisotropy ($\kappa_{ab}/\kappa_c$) in the thermal conductivity can be seen,

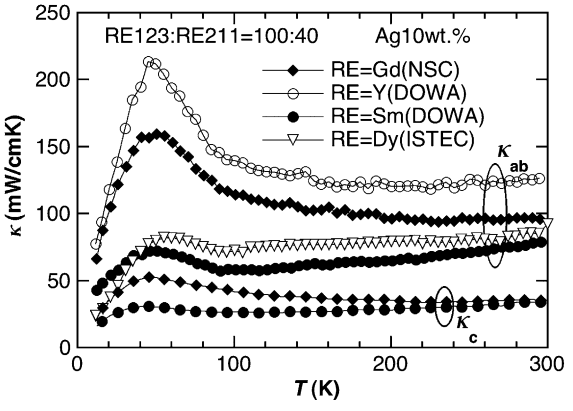


Fig. 1. The *ab*-plane thermal conductivity $\kappa_{ab}(T)$ for various kinds of bulks with the RE211 contents of $X = 40$, adding the Ag metal of 10 wt.%.

which is reduced with increasing Ag contents [3]. The temperature dependence and the absolute value of $\kappa_{ab}$ change depending on the species of RE ion; for the Sm- and Dy-systems, the $\kappa_{ab}(T)$ enhancement below the superconducting transition temperature $T_c$ and the absolute value above $T_c$ is fairly small. For the light RE (LRE) element such as Sm and Nd, a part of the LRE ions is substituted for the Ba site, thus forming the $LRE_{1+y}Ba_{2-y}Cu_3O_z$-type solid solution. The migration of Sm and Ba decreases in oxygen-reduced atmosphere but a small amount of the migration remains. The migration enhances the phonon scattering in the Sm123 phase, working as a kind of point-defect-type phonon scattering centers. On the other hand, for the RE = Y and Gd systems, $\kappa_{ab}(T)$ shows a large enhancement below $T_c$. The absolute $\kappa_{ab}(T)$ value is large with the negative $d\kappa_{ab}/dT$ slope which suggests that no migration of RE and Ba takes place and a good crystalline RE123 phase can be confirmed from the heat transport. It should be noticed that, for the Dy-system, a very small $\kappa_{ab}(T)$ can be observed comparable with the Sm-system. The Dy-system has been considered to be the non-substituted system of Dy ions for the Ba site because the ionic radius of $Dy^{3+}$ is large comparable with $Y^{3+}$. A sizable amount of the migration of Dy and Ba may take place or other powerful phonon scattering centers may be introduced. A detailed investigation is in progress.

Fig. 2 shows the temperature dependence of the *ab*-plane thermoelectric power $S_{ab}(T)$ for the same bulks shown in Fig. 1. In the normal state, the $S_{ab}(T)$ value for the Y-system is negative, but that for the Sm-system is positive. Quantitatively, $S$ is expected to increase in materials with some kinds of defects because of increasing resistivity $\rho$ values. In the $YBa_2Cu_3O_{7-\delta}$ phase, the $S$ value continuously changes from negative to positive with increasing oxygen deficiency $\delta$, which also reflects the $\rho$ values [10]. In the Sm system, the observed $S_{ab}$ increases positively with increasing $X$ [3], which may partly be attributable to the $\rho_{ab}(T)$ increase in the Sm123 phase caused by the migration effect and/or the increase of the oxygen deficiency $\delta$. The large negative $S_{ab}$ value of the Y-system suggests that no substitution of $Y^{3+}$ for the $Ba^{2+}$

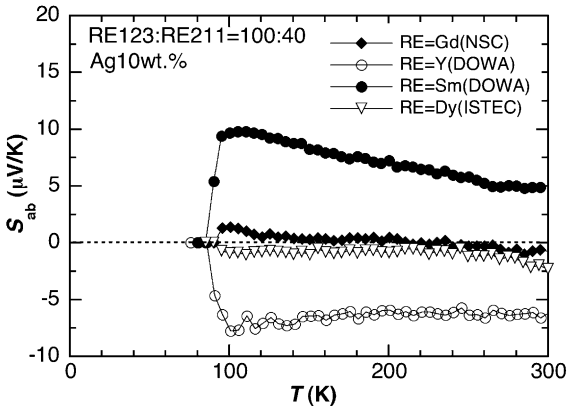


Fig. 2. The *ab*-plane thermoelectric power $S_{ab}(T)$ for the same bulks shown in Fig. 1.

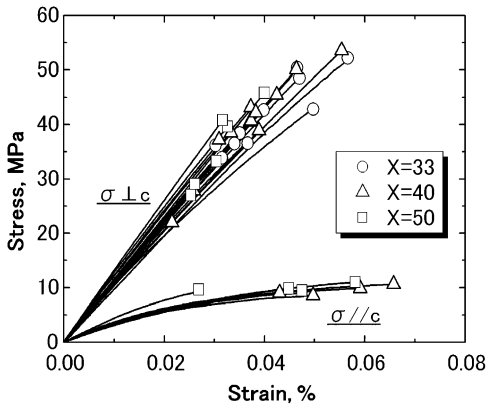


Fig. 3. The effects of Gd211 contents $X$ on tensile stress–strain behavior of Gd-bulk (NSC) by stressing ($\sigma$) in *c*-axis and perpendicular to *c*-axis at RT. Symbols indicate fracture points.

site and the sufficient oxidation ($\delta = 0$) should take place during the fabrication processes [10]. On the other hand, for the Gd- and Dy-systems, $S_{ab}$ value is nearly zero. Since the present bulk materials are a composite system, we cannot analyze $S_{ab}(T)$ at the present stage. However, it is worth while to note that the migration effect can be detected by the $S_{ab}(T)$ measurements, if the oxygen content is nearly equal.

### 3.2. Mechanical properties [4,11–20]

Typical stress–strain curves for the Gd-system with different Gd211 contents ($X = 33, 40, 50$) and 10 wt.% $Ag_2O$ loaded in the *c*-axis direction or perpendicular to it at room temperature (RT) are shown in Fig. 3 [11,12]. The latter was almost linear until the fracture, while the former was not. This anisotropy is mainly ascribed to the opening of the pre-existing micro-cracks perpendicular to the *c*-axis formed during the fabrication process. The Young's modulus ($E$) for the latter was 100–130 GPa and that for the former was 35–45 GPa. It increased with increase of the Gd211 contents $X$. The tensile strength in the direction perpendicular to the *c*-axis was 20–55 MPa and that in the *c*-axis was about 10 MPa. The former decreased with increase of $X$. The fracture surface observations clarified that the crack initiates from voids or sub-grains [13,14]. There was a significant anisotropy in the Poison's ratio due to the micro-cracks; the value for loading perpendicular to the *c*-axis were 0.15 for the transverse strain in the *c*-axis, and 0.30–0.36 for that perpendicular to it [11]. The specimen length dependence of the elastic constants observed was ascribed to the constraints near the interfaces between the specimen and the aluminum alloy rods [11].

The compressive stress–strain curves in perpendicular to the *c*-axis were almost linear, while those in the *c*-axis were non-linear; increasing with increase of the applied stress [15]. This can be ascribed to the closure of the pre-existing micro-cracks. The $E$ defined from the region of the almost linear part of the stress–strain curves (after the closure of the pre-existing micro-cracks) in the *c*-axis was smaller than those in perpendicular to the *c*-axis. This is considered to be originated from the intrinsic anisotropy of the bulk. The compressive strength in the *c*-axis was higher than that in the perpendicular to the *c*-axis. This is ascribed to the buckling fracture associated with the pre-existing micro-cracks perpendicular to the *c*-axis in the loading perpendicular to the *c*-axis. Both of the $E$ and the fracture strength by compressive test were higher than those by tensile test [15].

The $E$ and strength $\sigma_f$ by bending tests of the Y- and Gd-bulks at RT and liquid nitrogen temperature (LNT) are shown in Fig. 4 [16,17]. The Y-bulk ($X = 33$, Ag: 0, NSC), Y-bulk ($X = 40$, Ag: 15 wt.%, DOWA) and Gd-bulk ($X = 33$, Ag:

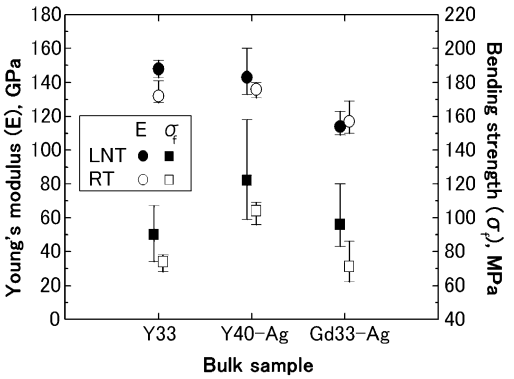


Fig. 4. The bending mechanical properties of Y33-, Y40-Ag- and Gd33-Ag-bulks at RT and LNT (see text).

10 wt.%, NSC) are denoted as Y33, Y40-Ag and Gd33-Ag, respectively. The $E$ of Y33 and Y40-Ag at LNT, 148 and 143 GPa were higher than those at RT, 132 and 136 GPa, respectively. This temperature dependence coincides with theoretical ones [11] associated with the inter-atomic distance. The $E$ at RT was higher than that by tensile test [12]. This can be ascribed to the behavior of the compressive stress region induced in a half of the volume of the bending test specimens. The $\sigma_f$ of Y33, Y40-Ag and Gd33-Ag at LNT, 90, 122 and 96 MPa, were higher than those at RT, 74, 104 and 71 MPa, respectively. The bending fatigue endurance limits of the Y33 and that of the Gd33-Ag for $5 \times 10^4$ stress cycles at LNT were about 80% and 70% of $\sigma_f$, respectively [16,17].

The fracture toughness $K_{Ic}$ for the bulks ranged from 1.0 to 2.0 MPa $m^{1/2}$ [4,18–20]. Although, the $K_{Ic}$ obtained from bending tests and tensile tests coincided fairly well, those from indentation test gave underestimation [18]. While the Vickers hardness increased with lowering temperature, the $K_{Ic}$ from indentation decreased and those from notched specimen increased [4,18,20].

## 4. Summary

The thermal properties and mechanical properties have been measured at low temperatures and under a high magnetic field for about 50 REBaCuO bulks. The database of these properties has been constructed and opened on the Web site. The influence of the species of RE ions, the content, size and dispersion of the RE211 phase and Ag metals and defects distribution on these properties is characterized in the database. We expect that the database will be widely used for the practical application and the basic research for the REBaCuO bulks.

## Acknowledgements

The authors greatly thank Dr. S. Kohayashi of Dowa Mining Co., Ltd., Dr. H. Teshima of Nippon Steel Co., Ltd., Dr. S. Nariki and Dr. N. Sakai of ISTEC for the sample preparation and valuable discussion. We also thank Prof. M. Murakami of Shibaura Institute of Technology for the technical support and valuable suggestion. This work is partially supported by Japan Science and Technology Corporation under the Joint-research Project for Regional Intensive in the Iwate Prefecture on "development of practical applications of magnetic field technology for use in the region and in everyday living".

## References

[1] M. Ikebe, H. Fujishiro, T. Naito, K. Noto, J. Phys. Soc. Jpn. 63 (1994) 3107.
[2] H. Fujishiro, M. Ikebe, S. Kohayashi, K. Noto, K. Yokoyama, Cryogenics 43 (2003) 477.
[3] H. Fujishiro, S. Kohayashi, IEEE Trans. Appl. Supercond. 12 (2002) 1124.
[4] Y. Yoshino, A. Iwabuchi, K. Katagiri, K. Noto, N. Sakai, M. Murakami, IEEE Trans. Appl. Supercond. 12 (2002) 1755.
[5] K. Noto, T. Itoh, A. Sugiyama, M. Murakami, M. Muralidhar, J. Yoshioka, T. Kikegawa, N. Kobayashi, Physica C 335 (2000) 97.
[6] H. Fujishiro, M. Ikebe, K. Noto, H. Teshima, M. Sawamura, J. Cryo. Soc. Jpn. 37 (2002) 659 (in Japanese).
[7] H. Fujishiro, H. Teshima, M. Ikebe, K. Noto, Physica C 392–396P1 (2003) 171.
[8] K. Noto, T. Oka, K. Yokoyama, K. Katagiri, H. Fujishiro, H. Okada, H. Nakazawa, M. Muralidhar, M. Murakami, Physica C 392–396P1 (2003) 677.
[9] H. Fujishiro, M. Ikebe, T. Naito, K. Noto, Jpn. J. Appl. Phys. 33 (1994) 4965.
[10] P.J. Ouseph, M.R. O'Bryan, Phys. Rev. B 41 (1990) 4123.

[11] A. Murakami, K. Katagiri, K. Kasaba, Y. Shoji, K. Noto, H. Teshima, M. Sawamura, M. Murakami, Cryogenics 43 (2003) 345.
[12] K. Katagiri, A. Murakami, Y. Shoji, H. Teshima, M. Sawamura, A. Iwamoto, T. Mito, M. Murakami, Physica C 412–414 (2004) 633.
[13] K. Katagiri, K. Kasaba, Y. Shoji, A. Chiba, M. Tomita, T. Miyamoto, M. Murakami, Physica C 357–360 (2001) 803.
[14] A. Murakami, K. Katagiri, K. Kasaba, Y. Shoji, K. Noto, N. Sakai, M. Murakami, Supercond. Sci. Technol. 15 (2002) 1099.
[15] R. Kan, K. Katagiri, A. Murakami, K. Kasaba, Y. Shoji, K. Noto, N. Sakai, M. Murakami, IEEE Trans. Appl. Supercond. 14 (2004) 1114.
[16] A. Murakami, K. Katagiri, K. Kasaba, K. Noto, H. Teshima, M. Sawamura, N. Sakai, M. Murakami, Physica C 412–414 (2004) 673.
[17] A. Murakami, K. Katagiri, K. Kasaba, Y. Shoji, K. Noto, H. Teshima, M. Sawamura, M. Murakami, IEEE Trans. Appl. Supercond. 14 (2004) 1050.
[18] K. Katagiri, A. Murakami, T. Okudera, Y. Yoshino, A. Iwabuchi, K. Noto, N. Sakai, M. Murakami, IEEE Trans. Appl. Supercond. 14 (2004) 1046.
[19] T. Okudera, A. Murakami, K. Katagiri, K. Kasaba, Y. Shoji, K. Noto, N. Sakai, M. Murakami, Physica C 392–396 (2003) 628.
[20] Y. Yoshino, A. Iwabuchi, N. Takahashi, K. Katagiri, K. Noto, N. Sakai, M. Murakami, IEEE Trans. Appl. Supercond. 14 (2004) 1118.